Colloid Polym Sci 274:1–7 (1996)

ORIGINAL CONTRIBUTION

M. Lukaschek
S. Müller
A. Hansenhindl
D.A. Grabowski
C. Schmidt

Lamellar lyomesophases under shear as studied by deuterium nuclear magnetic resonance

Received: 11 August 1995
Accepted: 17 August 1995

M. Lukaschek · S. Müller
A. Hasenhindl · Dr. C. Schmidt (✉)
Institut für Makromolekulare Chemie
Universität Freiburg
Sonnenstraße 5
79104 Freiburg

D.A. Grabowski
Freiburger Materialforschungszentrum
Universität Freiburg
Stefan Meier Straße 21
79104 Freiburg

Abstract The lamellar phases of two aqueous ethylene oxide surfactants, tetra(ethylene oxide) dodecyl ether and hexa(ethylene oxide) dodecyl ether, have been investigated by deuterium nuclear magnetic resonance spectroscopy during shear. The evolution of the shear-induced NMR line shapes and their dependence on surfactant concentration, shear geometry and shear history is analyzed. Two of three previously described shear-induced states (Diat O, Roux D, Nallet F (1993) J Phys II France 3: 1427–1452), namely the state of aligned lamellae with the layer normal parallel to the velocity gradient, which occurs at low shear rates, and the vesicular state at intermediate shear rates are found and identified by their characteristic NMR line shapes.

Key words NMR – nonionic surfactant – lamellar phase – shear-induced structure

Introduction

Surfactants in aqueous solution have been known for a long time to form a variety of liquid-crystalline phases [1]. With increasing surfactant concentration, cubic (I_1), hexagonal (H_1), bicontinuous cubic (V_1), and lamellar (L_α) phases may occur. The formation of these phases is governed essentially by geometric constraints as described by the packing parameter introduced by Israelachvili et al. [2]. The packing parameter determines the curvature of the hydrophobic/hydrophilic interface and thus the shape of the micellar aggregates and the phase structure. While the equilibrium phase diagrams are fairly well understood, little is known about non-equilibrium shear-induced structures in the concentration regime of the liquid-crystalline phases.

In the past, most rheological studies of surfactant systems have focused on the low concentration micellar regime. Investigations of the flow properties of the lyomesophases, which occur at higher surfactant concentrations, are scarce but growing in number. Since the earliest studies of lamellar surfactant mesophases, their rheological complexity has been known [3–16]. The rheological properties generally depend on the mechanical pretreatment of the samples [3, 7, 14, 16], indicating that shear induces orientations or structures that show slow, if any, relaxation. Most L_α phases can be characterized as plastic fluids with a yield stress [5, 7, 10] that has been reported to decrease when measurements are repeated on the same sample [7]. Diagrams of shear stress vs. shear rate can show both thixotropic and rheopectic (anti-thixotropic) hysteresis loops [3, 4, 14]. The same sample may exhibit both types of behavior, depending on its shear history [14]. Studies of lamellar systems are further complicated by the fact that their response to shear depends on the sample thickness [6, 12, 15]. Viscosity measurements on an oriented lamellar phase between parallel plates with gap sizes up to 500 μm showed an increase of viscosity with sample thickness, an observation that was ascribed to the quenching of undulation forces by the plate surfaces [6].

Since macroscopic rheological measurements alone do not reveal structural details of sheared samples, explanations for the observed phenomena remain mostly speculative when based merely on rheological data. To analyze the shear-induced structures and orientations that give rise to the macroscopic properties, techniques providing microscopic information, such as birefringence and scattering measurements, are in demand. A recent study of sheared L_α phases by light and neutron scattering and polarizing microscopy [11–13] has shown the existence of three distinct flow regimes. An isotropic state where the bilayers form multi-lamellar vesicles (onion-like structures) occurs at intermediate shear rates, whereas at lower and higher shear rates two other states are observed in which the layers align mainly parallel to the flow. While light scattering probes structures at a micrometer scale, that is, well above the typical lamellar period, both neutron scattering and nuclear magnetic resonance (NMR) can be used to study the phase structure on the molecular level. In particular, deuterium NMR of D_2O-enriched surfactant/water mixtures is a well established method for the study of surfactant phase diagrams and the microstructure of the different phases. This technique probes the motionally averaged electric quadrupole couplings between the deuterium nuclei (spin $I = 1$) and the electric field gradient. The residual couplings arise from the anisotropy of the rotational motions of the water molecules and thus depend on the curvature of the hydrophobic/hydrophilic interface. In order to use NMR for the study of shear-induced orientations and structures, we designed shear cells for use in a conventional NMR probe for a superconducting magnet. Results obtained with a cone-and-plate cell (which enables the simultaneous measurement of viscosity) for a thermotropic side-chain liquid-crystalline polymer [17] and for a hexagonal surfactant mesophase [18] have been reported recently.

In this article we present first results from our rheo-NMR experiments on the L_α phases of two nonionic surfactants, $C_{12}E_4$ (recently also studied by rheo-small-angle light scattering [15]) and $C_{12}E_6$. In the notation C_nE_m, C_n symbolizes the hydrophobic n-alkyl group, C_nH_{2n+1}–, and E_m denotes the hydrophilic oligo(ethylene oxide) head group $-(OCH_2CH_2)_mOH$. We will demonstrate in the following that deuterium NMR is a powerful tool for the study of shear-induced changes of structure and orientation in lamellar lyomesophases.

Experimental

The surfactants, $C_{12}E_4$ and $C_{12}E_6$, were synthesized according to standard procedures [19]. Homogeneous mixtures with D_2O were obtained by shaking the samples in a vibrating mill in the isotropic phase. The phase diagram of $C_{12}E_4/H_2O$ shows a broad lamellar phase extending from very low surfactant concentrations to about 85 w/w % surfactant [1, 20]. The system $C_{12}E_6/H_2O$ forms a hexagonal, a bicontinuous cubic and a lamellar liquid crystalline phase, with the latter extending from about 60 to about 85 w/w % surfactant [20, 21].

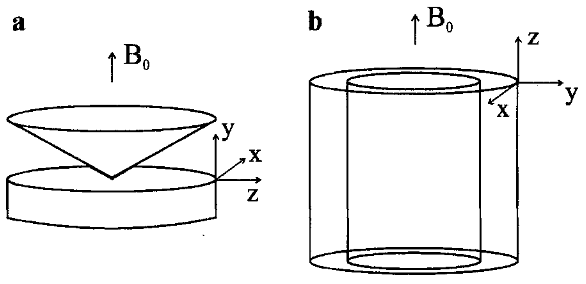

Fig. 1 Shear geometries used in the rheo-NMR experiments. For the cone-and-plate geometry (a) the shear plane, spanned by the velocity and the velocity gradient (xy plane), is parallel to the magnetic field, whereas for the Couette geometry (b) the shear plane is perpendicular to the magnetic field

The rheo-NMR measurements were performed in either a cone-and-plate cell or a Couette cell. Both geometries are depicted in Fig. 1. For the cone-and-plate cell, which has a diameter of 15 mm and a gap angle of 5°, the velocity (x) is perpendicular and the velocity gradient (y) is parallel to the magnetic field. With this cell viscosities can be measured simultaneously with the NMR spectra [17, 18]. Unlike the cone-and-plate NMR cell built by Nakatani et al. [22], our cell cannot be rotated with respect to the magnetic field. To be able to identify shear-induced orientations unequivocally, we constructed another cell having coaxial-cylinder geometry (Couette), for which the shear plane is perpendicular to the magnetic field. This Couette cell has an outer diameter of the inner cylinder of 5.1 mm and a gap of 0.3 mm. An advantage of the Couette cell is the fact that solvent evaporation during the measurement is negligible. Solvent evaporation, which can be detected easily by measuring the intensity of the deuterium NMR signal as a function of time, is a problem for measurements in the cone-and-plate cell because a large part of the sample surface is exposed to the flow of nitrogen gas used for thermostatting. As demonstrated previously [18], water evaporation can be delayed by coating the surface of the sample with a thin film of $N(n\text{-}C_4F_9)_3$. This perfluorinated amine has a boiling point of 437 K and shows very poor solubility in the surfactant/water mixture so that evaporation of D_2O is delayed by approximately 2.5 h, depending on temperature and N_2 flow.

For both types of shear cells saddle-type radiofrequency NMR coils are used, which have small filling factors. The 90° pulse durations are approximately 15 μs and 8 μs for the cone-and-plate and the Couette cell, respectively. Deuterium NMR spectra were obtained with Bruker CXP and MSL 300 spectrometers at a resonance frequency of 46.07 MHz using a phase-cycled quadrupole echo sequence with 90° pulses and a delay of 40 μs before the refocusing pulse. Typically 100–200 scans were acquired for one spectrum, with relaxation delays of 0.4–0.5 s between scans.

For each series of experiments, reproducible initial conditions were achieved by filling the sample into the gap, keeping it in the isotropic micellar phase to erase different shear histories that arise from stresses during the filling procedure, and bringing it slowly into the lamellar phase. If not noted otherwise measurements were carried out at 298 K. Since the transition from the isotropic to the lamellar phase takes place in the magnet, a macroscopic alignment of the domains in the sample results. One obtains polydomain samples with a planar distribution of the layer normal vectors (directors) in the plane perpendicular to the magnetic field, since oligo(ethylene oxide) alkyl ether surfactants have a negative anisotropy of the diamagnetic susceptibility.

Results

Deuterium NMR spectra of the L_α phase of $C_{12}E_6$ in a mixture with D_2O, containing ca. 80 w/w % surfactant, obtained under steady state shear conditions in the cone-and-plate cell, are shown in Fig. 2. The shear rates are given in s^{-1} to the right of each spectrum. The first spectrum at zero shear rate corresponds to the magnetically aligned state mentioned above that is obtained by slow cooling from the isotropic phase. The doublet with a quadrupole splitting of 1.6 kHz corresponds to an angle of 90° between the layer normal and the magnetic field. Due to the rapid but anisotropic rotational motions of the water molecules in the uniaxial lamellar phase the residual quadrupole coupling results in a line splitting $\Delta\nu$ given by

$$\Delta\nu = \frac{3}{4}\delta(3\cos^2\theta - 1)\,, \qquad (1)$$

where θ is the angle between the director and the magnetic field and $\delta = e^2qQ/h$ is the motionally averaged quadrupole coupling constant. According to Eq. (1), the deuterium NMR line shape depends on the orientational distribution of directors. As can be seen from the change of line shapes with increasing shear rate, shown in Fig. 2, shear causes dramatic changes of the director distribution function. The increasing intensity at the maximum quadrupole splitting, corresponding to $\theta = 0°$, proves that up to a shear rate of about $0.02\,s^{-1}$ more and more layers become aligned with their normal parallel to the magnetic field. Between shear rates of 0.02 and $3.2\,s^{-1}$ a fairly stable state of orientation exists where the line shapes do not change significantly. These spectra with maximum intensity at the frequencies corresponding to $\theta = 0°$ arise from a state of orientation, in which the lamellae are preferentially aligned perpendicular to the velocity gradient, that is, the layer normals are parallel to the velocity gradient, which is parallel to the magnetic field for the cone-and-plate geometry. The shear-induced alignment, however, is not perfect as can be inferred from the line shapes: the spectra are not simple doublets but have a relatively high intensity at frequencies corresponding to orientations with $\theta \neq 0°$. This shows that the structure has many defects with arbitrary orientations.

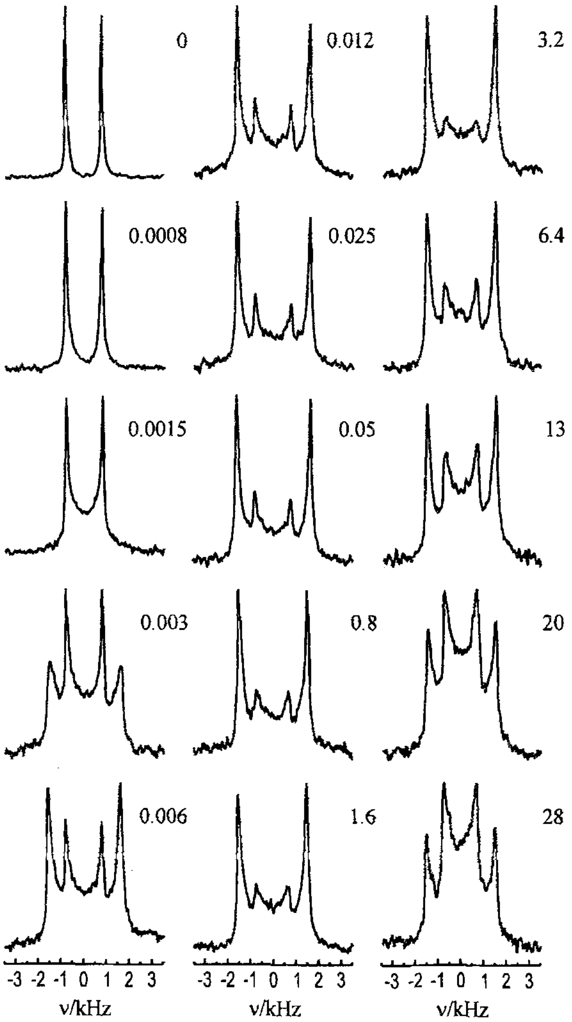

Fig. 2 Deuterium NMR spectra of $C_{12}E_6/D_2O$ (80 w/w % surfactant) at different shear rates in the cone-and-plate cell at a temperature of 292 K. The shear rates (in s^{-1}) are given to the right of the spectra

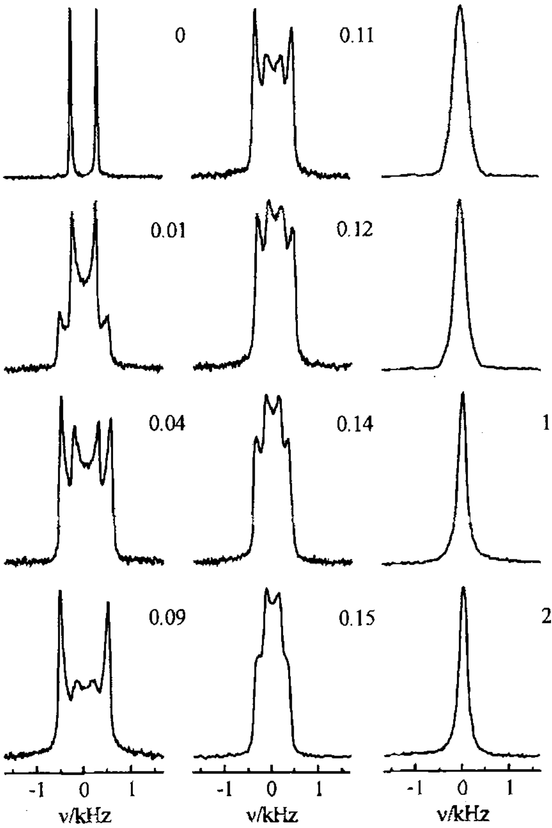

Fig. 3 Deuterium NMR spectra of $C_{12}E_4/D_2O$ (35 w/w % surfactant) at different shear rates in the cone-and-plate cell. The shear rates (in s^{-1}) are given to the right of the spectra

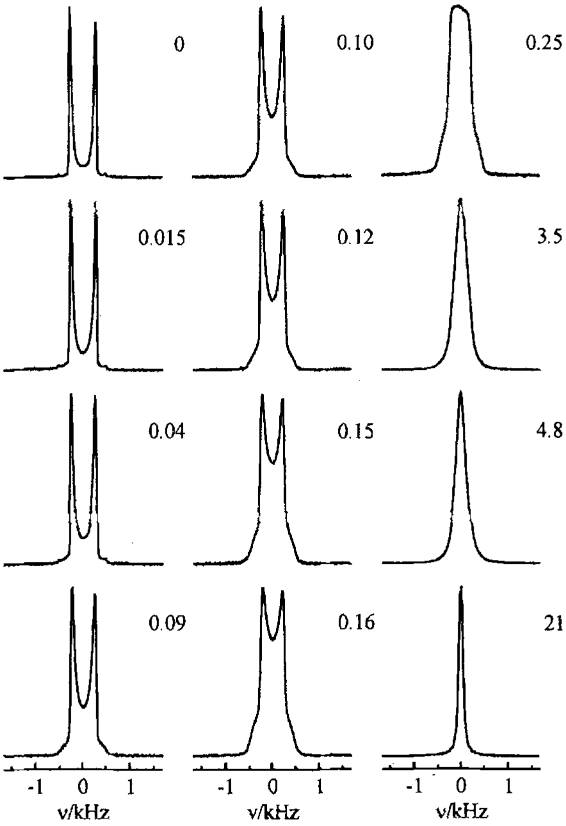

Fig. 4 Deuterium NMR spectra of $C_{12}E_4/D_2O$ (35 w/w % surfactant) at different shear rates in the Couette cell. The shear rates (in s^{-1}) are given to the right of the spectra

When the sample is sheared at rates higher than about $3\ s^{-1}$, a second transition to another flow regime is observed (cf. Fig. 2). The line shapes at shear rates between $3\ s^{-1}$ and $30\ s^{-1}$ show an increase of the inner 90° singularities at the expense of the outer 0° singularities. Since higher shear rates were not accessible with the cone-and-plate cell at the time when the experiments on the $C_{12}E_6$ system were performed, we cannot decide whether the spectra observed at the highest shear rates correspond to a stable state of orientation or still to the transition regime.

A closer inspection of the NMR spectra in Fig. 2 reveals that the total line width becomes smaller with increasing shear rate. The inner splitting decreases from 1600 Hz at shear rate zero to 1460 Hz at a shear rate of almost $30\ s^{-1}$. This decrease of the motionally averaged quadrupole coupling with increasing shear rate indicates that during the NMR experiment under shear the water molecules probe a more strongly curved surface by their lateral diffusion in the hydrophilic layer. This can be due to an increase of undulation or to a decrease of the lateral extension of defect-free flat layers as the sample is sheared at increasing rate.

Both shear-induced changes of the orientation state are correlated with a decrease of the apparent shear viscosity. Measurements in the cone-and-plate NMR cell, which yield only approximate values because of the coating with the fluorinated compound, show a drop in the apparent steady state viscosity by a factor of 10 from about 300 Pa s to 30 Pa s at shear rates between $0.0008\ s^{-1}$ and $8\ s^{-1}$, and a further decrease to about 1–2 Pa s at a shear rate of $28\ s^{-1}$.

Further experiments were performed with the surfactant system $C_{12}E_4/D_2O$, which shows a broader concentration range of the L_α phase. This system was investigated in both the cone-and-plate and the Couette cell at shear rates up to $120\ s^{-1}$ and $160\ s^{-1}$, respectively. The NMR spectra for sheared samples with ca. 35 w/w % $C_{12}E_4$ are depicted in Figs. 3 and 4 for the cone-and-plate and the Couette geometry, respectively. The sample is magnetically aligned by slow heating from the isotropic phase into the lamellar phase. The quadrupole splitting of 560 Hz in the quiescent state is much smaller than for the more concentrated $C_{12}E_6$ sample. This difference is mainly due to the larger thickness of the hydrophilic layer in the more dilute sample, which causes an, on average, less anisotropic environment of the individual water molecules.

At low shear rates up to 0.14 s^{-1}, the spectra obtained in the cone-and-plate cell (Fig. 3) evolve qualitatively in the same way as those for the $C_{12}E_6$ system. The first orientation state with flow-aligned layers preferentially in the *xz* plane is observed at shear rates around 0.09 s^{-1}. For the more dilute $C_{12}E_4$ mixture, the subsequent second transition starts at a much lower shear rate of 0.11 s^{-1} vs. 6 s^{-1} for the concentrated $C_{12}E_6$ sample. Figure 3 shows that the type of lineshape corresponding to that of the last spectrum in Fig. 2 undergoes further changes when the shear rate is increased. The most striking feature is a continuous rapid decrease of the quadrupole coupling until the splitting vanishes completely at a shear rate of 0.16 s^{-1} (not shown). The linewidth of the single peak continues to decrease with increasing shear rate.

The line shapes obtained in the Couette cell from the same sample (Fig. 4) confirm the observations made with the cone-and-plate cell. Since the shear plane is now perpendicular to the magnetic field, the spectra differ from those in Fig. 3. At low shear rates (below about 0.1 s^{-1} most layers are again oriented with their normal parallel to the velocity gradient, i.e., perpendicular to the magnetic field. Hence the line shapes are similar to that of the initial magnetically aligned state of orientation. However, shear-alignment is less perfect than magnetic alignment, as can be seen from the increasing intensity in the center of the spectra under shear. This is in agreement with the orientational disorder inferred from the spectra of Fig. 3 above. The spectra obtained with the Couette cell also show the transition to the second state of orientation, which is characterized by the single peak in the NMR spectra.

The final lineshapes observed for the dilute $C_{12}E_4$ sample at the highest shear rates do not change for several hours after shear has been terminated, indicating a very stable state of orientation. Samples in this state have been carefully transferred to a microscope stage. The images observed with crossed polarizers resemble those reported by Diat et al. [12], which have been ascribed to a dense packing of multilamellar vesicles.

To test whether the shear rate required for the transition to the second shear-induced state depends on the surfactant concentration as found by Roux and coworkers [11–13], the $C_{12}E_4$ system was also studied at a higher surfactant concentration of ca. 60 w/w %. This concentration corresponds approximately to the composition where the lamellar phase has its maximum thermal stability. The results obtained with the Couette cell are shown in Fig. 5. Except for the larger splitting of 1210 Hz, the same line shapes as in Fig. 4 are observed but, as expected, corresponding line shapes occur at higher shear rates for the more concentrated sample. Compared to the more dilute sample, the final orientation state with the single NMR peak is not as stable. The line shape changes after cessation of shear. This relaxation behavior is depicted in Fig. 6. Figure 6a shows the spectrum obtained during shear at a rate of 140 s^{-1} in the Couette cell and Fig. 6b and c show the line shapes observed at 1000 s and 15000 s, respectively, after shear has stopped. Upon cessation of shear a doublet with a splitting of 1190 Hz grows in the NMR spectrum, indicating that the structure relaxes back to the initial magnetically aligned plain lamellar state.

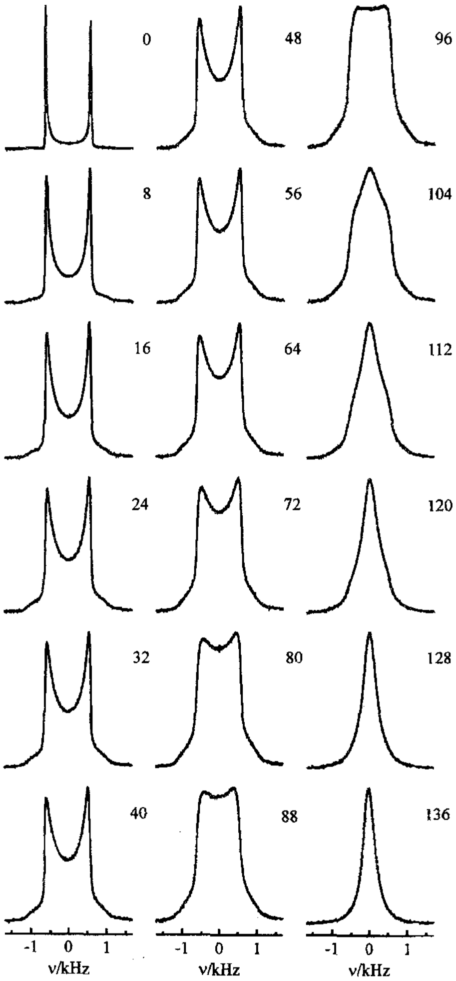

Fig. 5 Deuterium NMR spectra of $C_{12}E_4/D_2O$ (60 w/w % surfactant) at different shear rates in the Couette cell. The shear rates (in s^{-1}) are given to the right of the spectra

All the results shown so far are highly reproducible if the same shear history and geometry are applied. Caution is required, however, when results from measurements with different shear history or geometry are compared. An example for the influence of both geometry and history is shown in Fig. 7 for the 35 w/w % $C_{12}E_4$ sample. All three

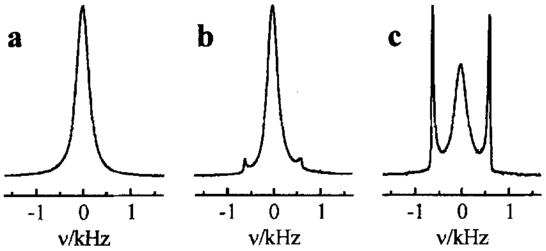

Fig. 6 Transformation of deuterium NMR line shape of $C_{12}E_4/D_2O$ (60 w/w % surfactant) after cessation of shear. a: During shear at a rate of 140 s^{-1}, b: 1000 s after shear has stopped, c: 15000 s after shear has stopped

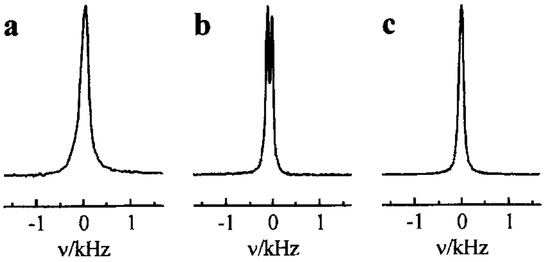

Fig. 7 Influence of shear history and shear geometry on deuterium NMR line shape of $C_{12}E_4/D_2O$ (35 w/w % surfactant). a: Cone-and-plate cell, after slow increase of shear rate to 20 s^{-1}, b: Cone-and-plate cell, after sudden jump in shear rate from 0 to 20 s^{-1}, c: Couette cell, after sudden jump in shear rate from 0 to 20 s^{-1}

spectra were obtained at the same shear rate of 20 s^{-1}. When the shear rate is slowly increased in the cone-and-plate cell, a broad single peak is observed (Fig. 7a). If, on the other hand, shear is started immediately at a high rate in the cone-and-plate cell, a spectrum with a splitting as in Fig. 7b results. Finally, if the same shear history is employed, but the Couette cell is used, one obtains the spectrum of Fig. 7c, which is again a single peak but with a smaller width. This example demonstrates the crucial dependence of the state of orientation on shear history and geometrical parameters like the gap size [6, 12, 15]. Note that the state corresponding to spectrum 7b is not stable but relaxes slowly, showing a decrease of the spectral splitting.

Discussion

From the NMR line shapes measured during shear we can clearly distinguish two different flow regimes, which are referred to as A and B in the following. Regime A shows a preferred orientation of the lamellae in the plane spanned by the velocity (x) and the vorticity (z) direction; the layer normal is parallel to the shear gradient (y). The structure has many defects which can be clearly seen from the line shapes of the deuterium NMR spectra. These findings for regime A are in perfect agreement with the observations by Roux and coworkers [11–13] who describe the first state of orientation as a shear-aligned lamellar structure with layers perpendicular to the velocity gradient and rich in defects. Regime B can be characterized by the occurrence of the single peak in the NMR spectra. Based on light and neutron scattering and polarizing microscopy, Roux and coworkers describe this second state as almost spherical multilamellar vesicles (also called onions) with a narrow size distribution. This is consistent with our NMR data. Translational diffusion in lamellar phases is highly anisotropic and restricted mainly to a given layer. Thus for large multilamellar vesicles a distribution of averaged quadrupole couplings is expected: while diffusion in the inner shells leads to isotropic averaging, diffusion in the outer shells covers only part of the sphere so that a residual coupling results. Superposition of spectra with different couplings yields the observed relatively broad but featureless lines. These considerations also explain why the linewidth decreases with increasing shear rate $\dot{\gamma}$: the vesicles become smaller. This was also observed by Roux and collaborators who found that the vesicle diameter scales with $\dot{\gamma}^{-1/2}$.

In agreement with Roux, we find that the vesicular state can be very stable. However, its stability depends on surfactant concentration. We find that the onion structure relaxes quickly at a concentration where the plain lamellar phase has high thermal stability and probably very few defects. A maximum of the quadrupole splitting is usually observed at that concentration [23]. The proposed relationship between equilibrium structure and stability of the shear-induced structure needs to be explored by further measurements.

Our data also confirm the shift of the transition from A to B to higher shear rates for samples with smaller lamellar period [11–13]. However, we have not yet observed the third state of orientation which, according to Roux, occurs at very high shear rates and consists of perfectly aligned layers. Even when shearing the 35 w/w % surfactant sample at 1000 or 2000 s^{-1} a single narrow peak results. This proves that neither extended layers nor any other large anisotropic structures are present. The observed NMR spectra are consistent only with small aggregates that allow nearly isotropic motion of the water molecules.

It should further be mentioned that Läuger et al. [15] who investigated the lamellar phase of aqueous $C_{12}E_4$ by rheo-small-angle light scattering in a parallel-plate cell find strongly anisotropic scattering patterns. They do not observe the nearly isotropic vesicular structures found by us and by Roux et al. This may be due to the fact that their measurements were performed at a surfactant concentration of 80 w/w %, in a region we have not yet analyzed by rheo-NMR.

The dynamic transition between flow regimes A and B appears to be continuous since the NMR line shapes change smoothly. For a first order transition a coexistence regime should occur, which is not observed for the systems studied. The transition to the third state of orientation, which is not observed here, on the other hand, has been reported to be of first order [12].

Conclusions

Our results show that rheo-NMR reveals many details of the shear-induced structures and orientations that can occur in surfactant systems. The method is complementary to scattering techniques and direct microscopic observations. By NMR on sheared lamellar phases of nonionic surfactants, we could confirm the existence of two of the three flow regimes identified earlier for other lamellar systems. Further experiments are necessary to investigate whether the lamellar structure of the third regime at very high shear rates [11–13] can be verified. A more detailed line shape analysis will yield details about the transitions between different regimes.

Acknowledgements We thank Martin Möller for stimulating the initial design of the Couette cell, Alexander Rössel for the lathe work, and the Deutsche Forschungsgemeinschaft for funding.

Reference

1. Tiddy GJT (1980) Phys Reports 57:1
2. Israelachvili JN, Mitchell DJ, Ninham BW (1976) J Chem Soc Faraday Trans II 72:1525
3. Solyom P, Ekwall P (1969) Rheol Acta 8:316
4. Groves MJ, Ahmad AB (1976) Rheol Acta 15:501
5. Tamamushi B, Kodaira Y, Matsumura M (1976) Colloid Polym Sci 254:571
6. Oswald P, Allain M (1988) J Colloid Interface Sci 126:45
7. Paasch S, Schambil F, Schwuger MJ (1989) Langmuir 5:1344
8. Muñoz J, Gallegos C, Flores V (1991) Tenside Surf Det 28: 204
9. Robles-Vasquéz O, Corona-Galván S, Soltero JFA, Puig JE (1993) J Colloid Interface Sci 160:65
10. Hoffmann H, Rauscher A (1993) Colloid Polym Sci 271:390
11. Diat O, Roux D (1993) J Phys II, France 3:9
12. Diat O, Roux D, Nallet F (1993) J Phys II, France 3:1427
13. Roux D, Nallet F, Diat O (1993) Europhysics Lett 24:53
14. Soltero JFA, Robles-Vasquéz O, Puig JE (1995) J Rheol (N.Y.) 39:235
15. Läuger J, Linemann R, Richtering W (1995) Rheol Acta 34:132
16. Franco JM, Muñoz J, Gallegos C (1995) Langmuir 11:669
17. Grabowski DA, Schmidt C (1994) Macromolecules 27:2632
18. Lukaschek M, Grabowski DA, Schmidt CS (1995) Langmuir 11:3590
19. Jahns E (1989) Diss Universität Freiburg
20. Klason T, Henriksson U (1984) In: Mittal KL, Lindman B (eds) Surfactants in Solution 1:93
21. Clunie JS, Goodman JF, Symons PC (1969) Trans Faraday Soc 65:287
22. Nakatani AI, Poliks MD, Samulski ET (1990) Macromolecules 23:2686
23. Schnepp W, Disch S, Schmidt C (1993) Liq Cryst 14:843